Considerations in 3D depth-specific P-S survey design

Don C. Lawton and Peter W. Cary†

ABSTRACT

A new sparse-shot design for 3D P-S surveys is introduced. In the sparse shot design a shot separation greater than the receiver separation is used, and given by the relationship $\Delta s = \Delta r(1 + Vp/Vs)/2$. This design yields fewer non-unique P-S traces than traditional 3D surveys with equal source and receiver intervals. New measures of global offset and azimuth distribution quality are developed which are tested in several design examples. These measures show that orthogonal and slant designs for P-S surveys yield similar design quality measures. An OBC survey example is also used to illustrate the efficacy of the sparse-shot design.

INTRODUCTION

In recent years, rising interest in converted-wave surveys, particularly ocean-bottom cable surveys has focused attention on multicomponent survey design. The primary problem in survey design is that the location of the conversion point is not well know *a priori*, even in geological environments in which reflectors are flat-lying. This contrasts with conventional P-P surveys where the reflection-point is always the source-receiver midpoint for horizontal reflectors and a flat recording surface or datum. Various studies (e.g. Yang and Lawton, 2002, 2003) have discussed P-S conversion-point dispersal as function of reflector depth, *Vp/Vs* in the overlying layers, anisotropy, and water depth (for OBC surveys). These effects all need to be considered at the survey design stage.

In this study, we examine the efficacy of orthogonal versus slant (i.e. oblique shot-line to receiver line) survey design for 3D P-S surveys, and propose a sparse shot approach to improve offset and azimuth uniqueness within common-conversion point (CCP) gathers. Figure 1 illustrates the P-S raypath from source to receiver for a flat reflector at a particular depth. In a layered medium, the conversion point follows a trajectory shown by the dashed line in Figure 1. For large offset-to-depth ratios, the conversion point moves towards the receiver, and at large depth-to-offset ratios, the conversion point approaches its asymptote given by (Tessmer and Behle, 1988):

$$x_c = \frac{x}{1 + Vs/Vp}$$

where x is the source-receiver offset and x_c is the offset of the asymptotic conversion point (ACP) from the source. For many years, converted-wave survey design was based on the ACP binning (e.g. Cordsen and Lawton, 1996; Cordsen, et al., 2000), partly because design software was not available for depth-variant P-S design, and partly because knowledge of *Vp/Vs* in sedimentary basins from the top down was poorly known, and thus more complex approaches to design were difficult.

† Sensor Geophysical Ltd., Calgary

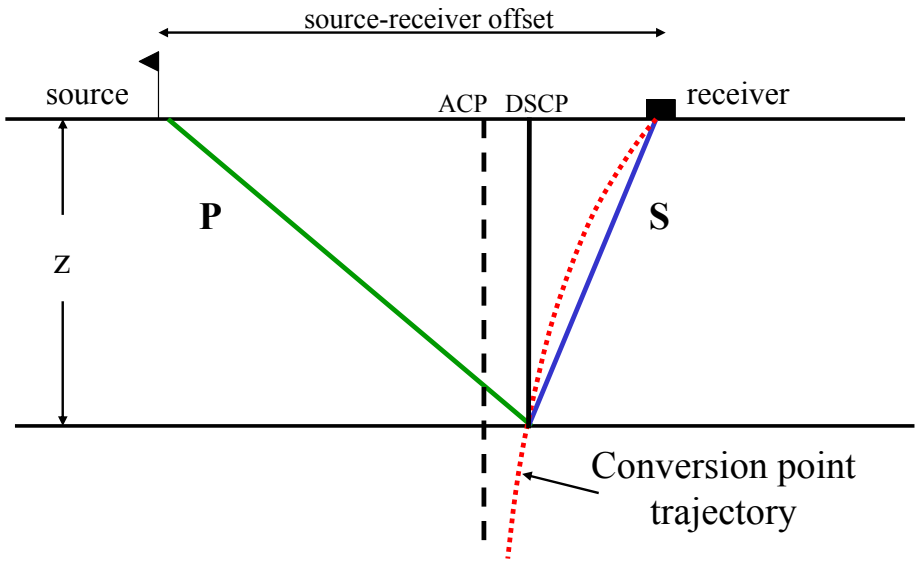

FIG. 1. P-S raypath geometry. ACP = asymptotic conversion point; DSCP = depth-specific conversion point.

ORTHOGONAL VERSUS SLANT DESIGN

Figure 2 shows a half-integer, orthogonal 3C-3D survey geometry with source and receiver line separations of 100 m, and source and receiver separations of 20 m.

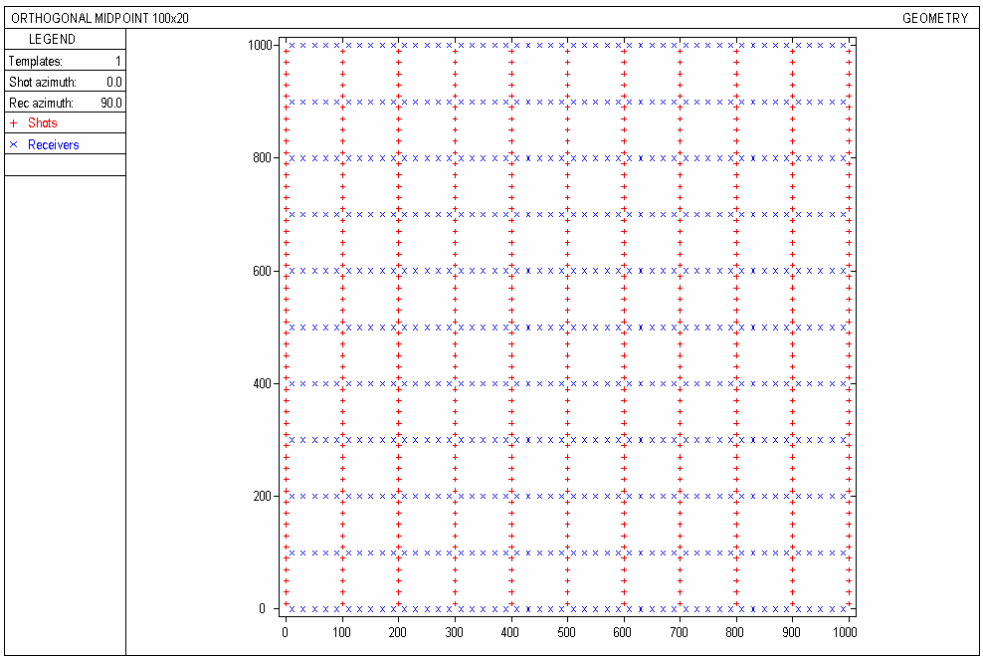

FIG. 2. Orthogonal Design A. Source interval = receiver interval = 20m. Shot-line interval = receiver-line interval = 100m.

Figure 3 illustrates the P-S fold calculated for this survey, assuming Vp/Vs = 2, source-receiver offsets up to 1000 m and ACP binning. As reported previously (e.g. Cary and Lawton, 2003), an artifact of ACP binning is the high spatial variability in P-S fold, in

some cases yielding empty bins. This undesirable fold pattern led to different design patterns aimed at smoother ACP fold maps. One approach was to use designs that result in distributed conversion points within bins such as 'Flexibin' (Cordsen and Lawton, 1996) or slanted shot lines (Musser, 2003; J. Schweigart, pers. comm), as illustrated in Figure 4.

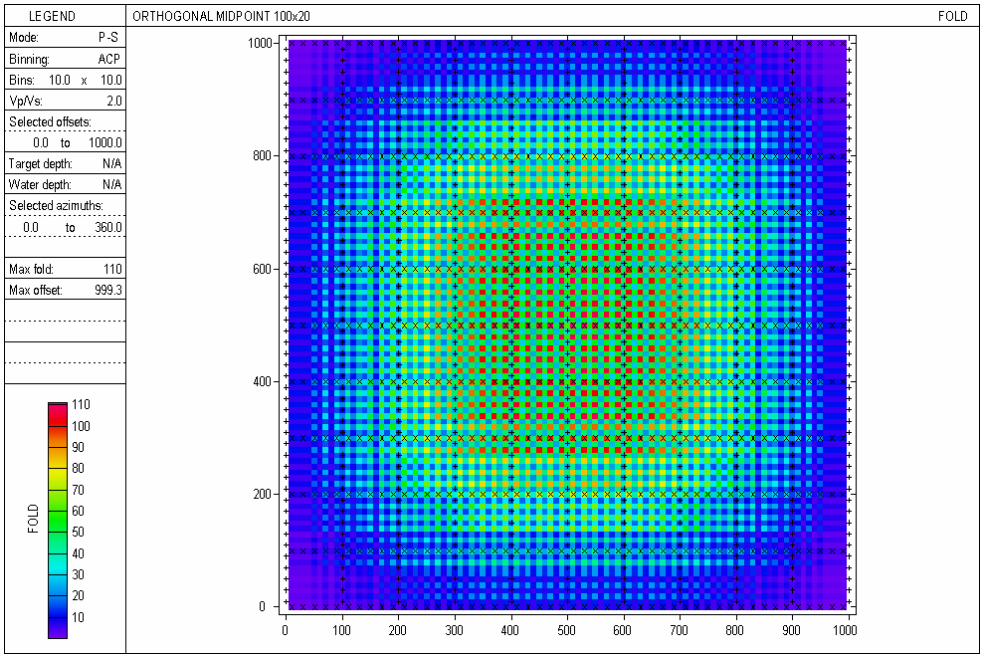

FIG. 3. P-S fold for Orthogonal Design A, asymptotic binning

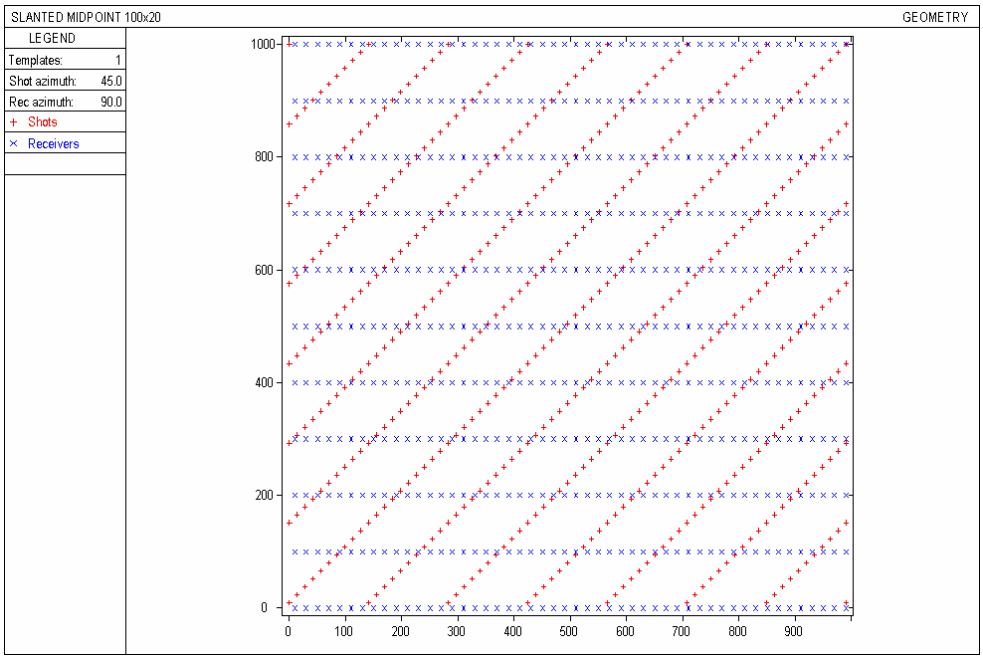

FIG. 4. Slant Design A. Source interval = receiver interval = 20m. Shot-line interval = receiver-line interval = 100m. Shot-line azimuth = 45^0; receiver-line azimuth = 90^0.

Figure 5 shows that the ACP P-S fold for a 45^0 slanted shot-line design is considerably smoother than that for the orthogonal design (Figure 3).

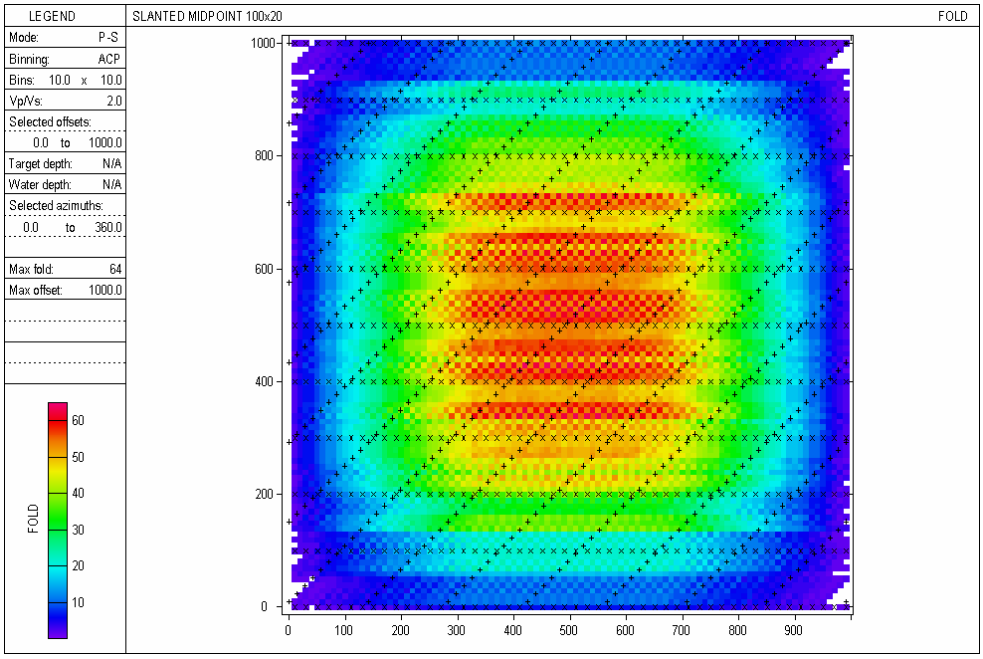

FIG. 5. P-S fold for Slant Design, asymptotic binning

Depth-specific conversion-point (DSCP) binning that honours the actual conversion point trajectory illustrated in Figure 2 yields P-S fold maps that generally have smoother fold than those produced with ACP binning. This is due to the scatter of conversion points throughout the bins. Furthermore, Cary and Lawton (2003) demonstrated that ACP P-S fold patterns change dramatically with only minor changes in *Vp/Vs* (e.g. 0.1), from which they concluded that interpolation is required to display meaningful illumination of the reflector at the target depth. They devised a sinc-function interpolator for band-limited seismic data (Figure 6).

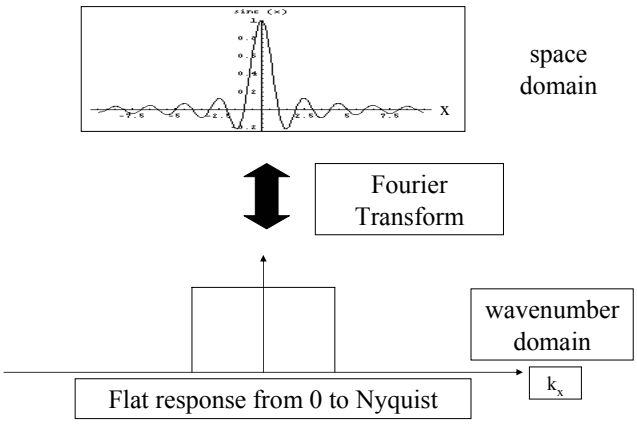

FIG. 6. Sinc-function interpolator used in P-S binning.

Figures 7 and 8 show interpolated depth-specific P-S fold at a target depth of 750m for orthogonal and slant designs, respectively, and Vp/Vs = 2.0. The similarity between these fold maps shows that both designs yield similar results in terms of reflector illumination.

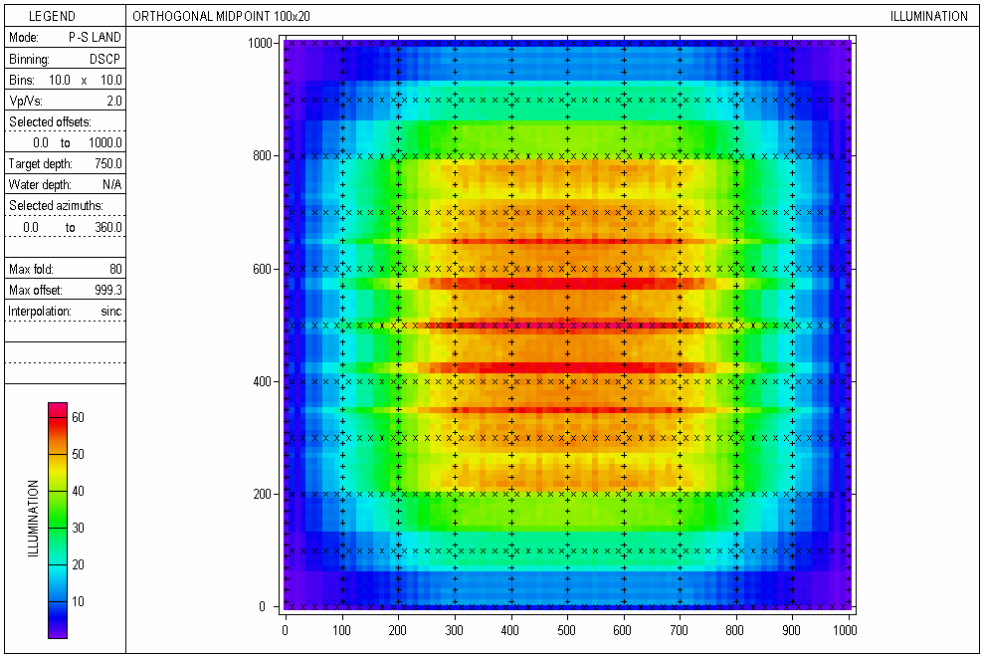

FIG. 7. P-S fold for Orthogonal Design A, interpolated, depth-specific binning

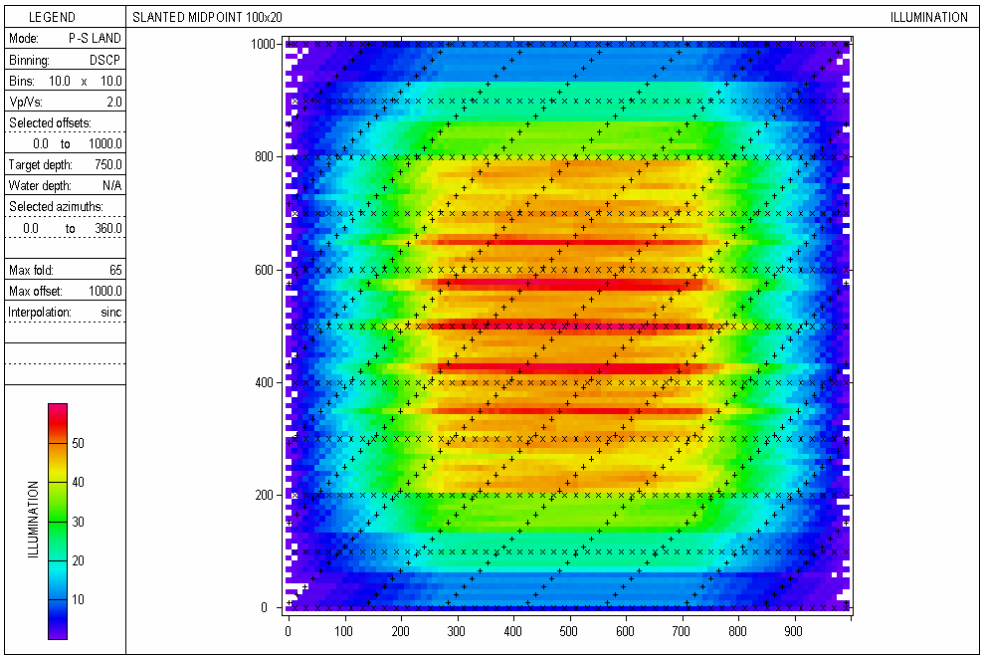

FIG. 8. P-S fold for Slant Design, interpolated, depth-specific binning

CROSS-LINE AND IN-LINE CONVERSION-POINT SEPARATION

An important observation was made when examining the geometry of traces contributing to any particular bin for orthogonal or slant designs in which the shot and receiver intervals are equal, and the binning interval is based on the P-P midpoint separation. Figure 9 shows many proximal traces from adjacent shots whose conversion points fall within the same CCP bin. Since these particular pairs of traces have very similar offsets and azimuths, the 'effective' fold within the bin will be reduced somewhat because source-generated coherent noise will not be attenuated in the stack.

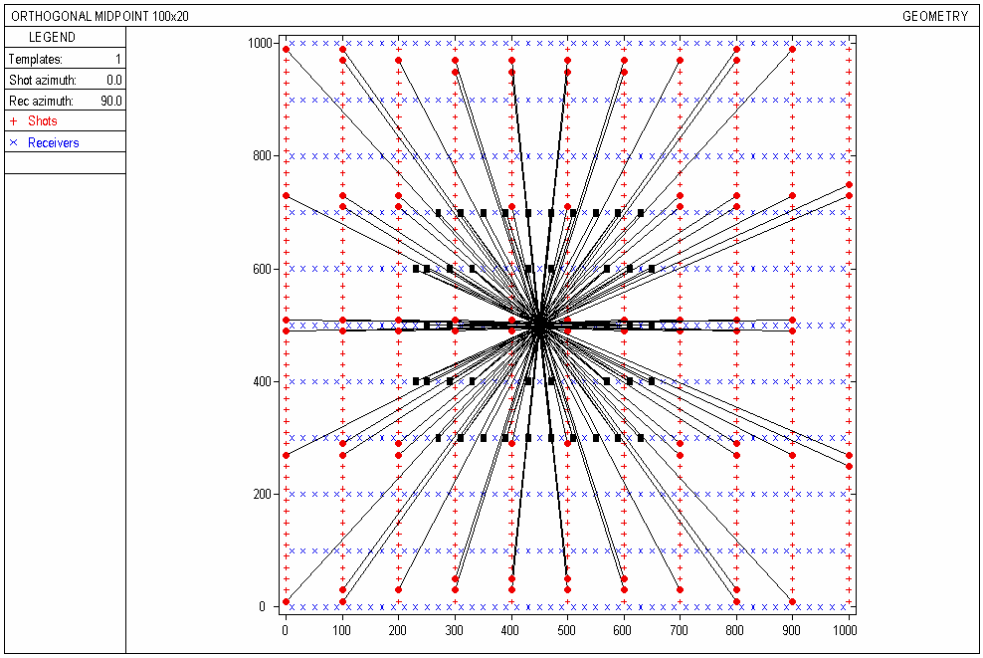

FIG. 9. Map view of P-S rays contributing to an arbitrary bin. Source-points are denoted by the red dots and receivers are denoted by the black rectangles. Note paired rays from adjacent shots.

The reason for the paired traces is evident from Figure 10 which compares the separation of conversion points in the common shot (in-line) direction (Δc_{inline}) with the separation of conversion points in the common receiver (cross-line) direction ($\Delta c_{crossline}$). These can be approximated in the asymptotic case by:

$$\Delta c_{inline} = \Delta r/(1+Vs/Vp)$$

$$\Delta c_{crossline} = \Delta s/(1+Vp/Vs)$$

where Δr and Δs are the receiver and shot separations, respectively. In depth-specific binning, the actual values of Δc the in-line and cross-line directions will not be exactly equal to the asymptotic values but will tend towards them for large depth/offset traces. A new approach to reduce the non-uniqueness issue for offset and azimuth statistics in a CCP bin is to use a 'sparse shot' design in which the shot interval is increased to:

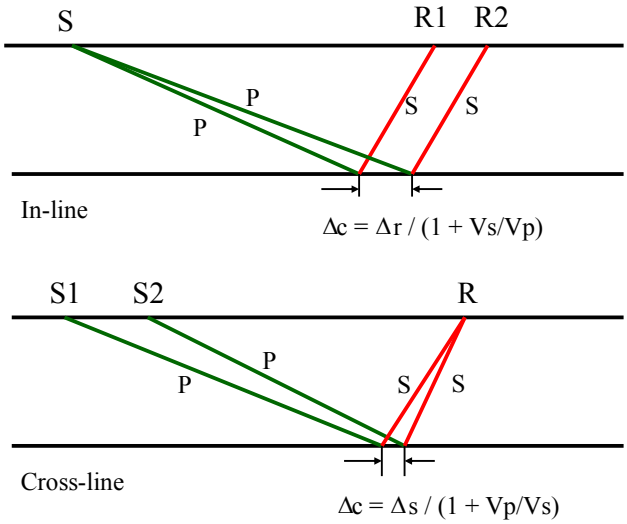

FIG. 10. In-line and cross-line separation of conversion points (asymptotic)

$$\Delta s = \frac{\Delta r}{2}\left(1 + Vp/Vs\right)$$

Thus, if $Vp/Vs = 2$, then $\Delta s = 3\Delta r/2$. However, to avoid orphaned or empty bins in the P-P data volume, consecutive shot lines must incorporate a shot stagger. Figure 11 illustrates an orthogonal design geometry that is similar to that in Figure 2 except that the shot interval has been increased to 30m, and a 10m shot stagger is added to each consecutive shot line.

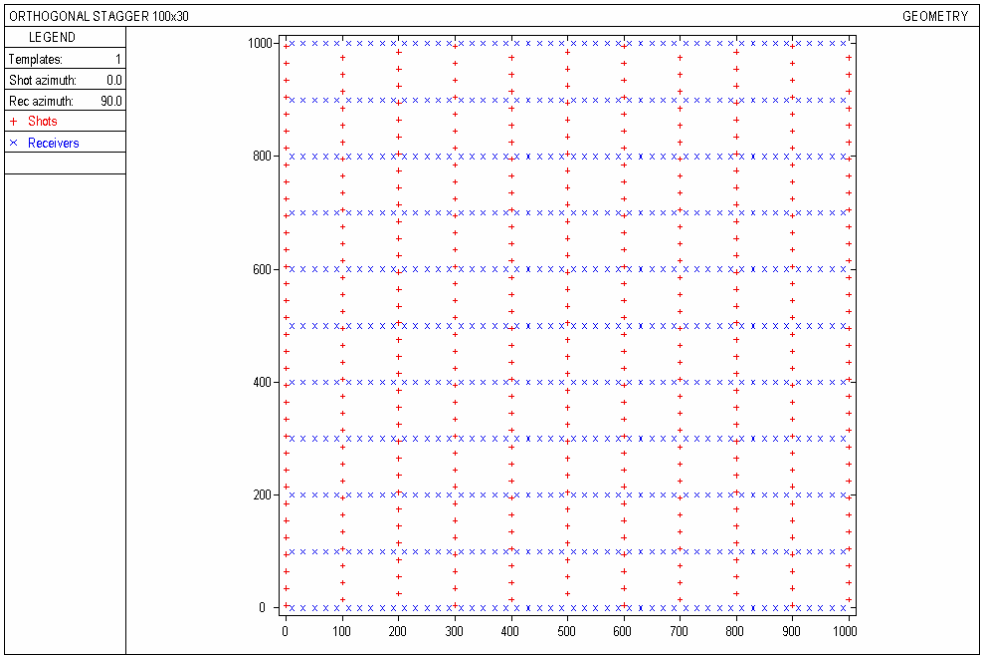

FIG. 11. Orthogonal Design B (sparse-shot). Source interval = 30m; shot stagger = 10m; receiver interval = 20m; shot-line interval = receiver-line interval = 100m.

Maps displaying P-P fold, depth-specific P-S fold, and interpolated P-S fold for this geometry are shown in Figures 12, 13 and 14 respectively.

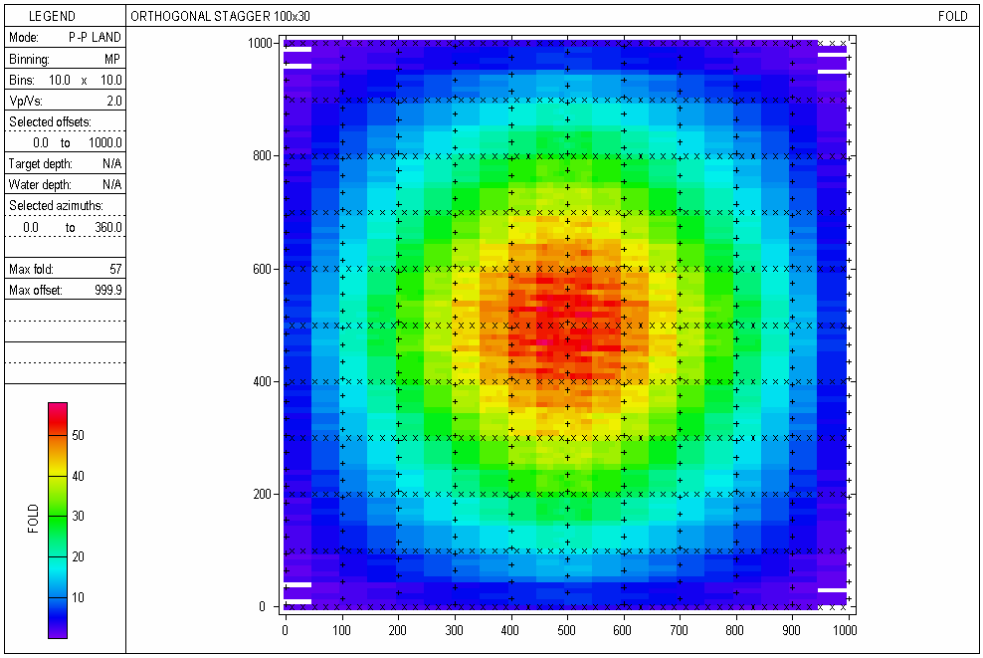

FIG. 12. P-P fold for Orthogonal Design B (sparse shot).

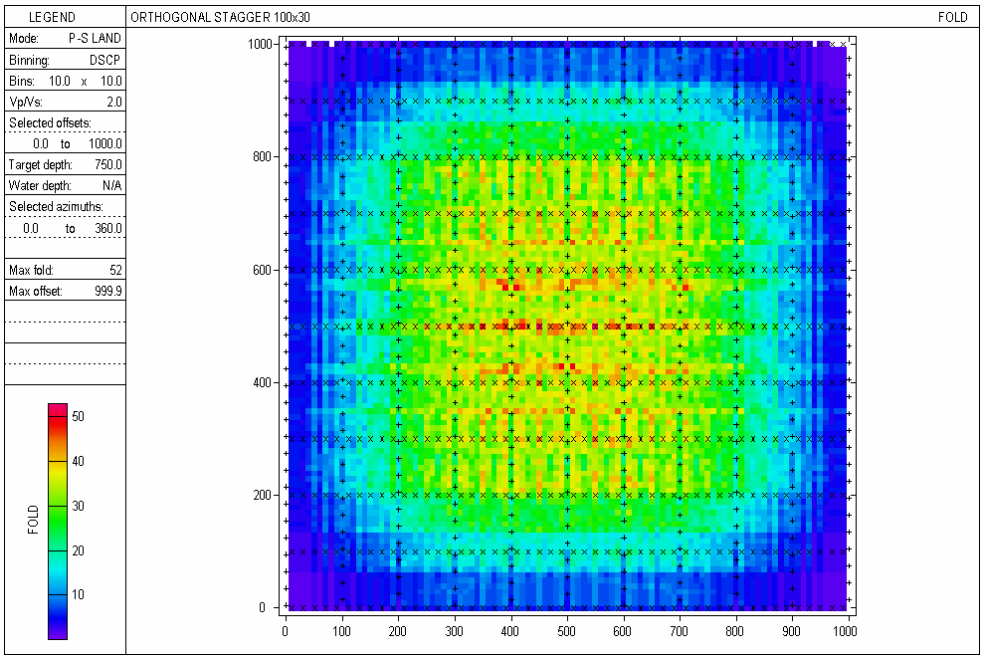

FIG. 13. P-S fold for Orthogonal Design B (sparse shot), depth-specific binning

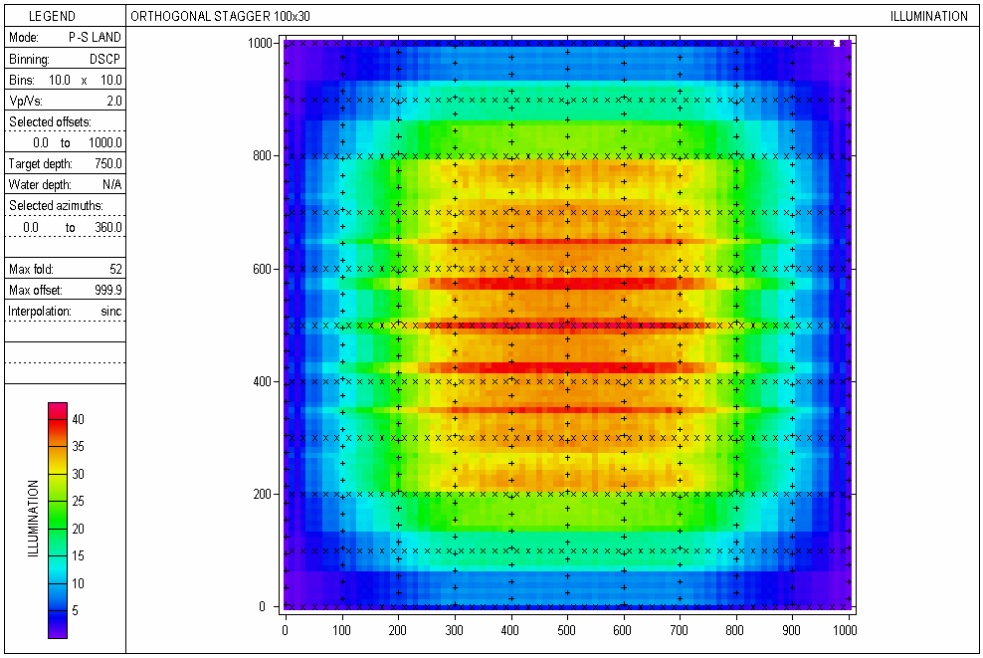

FIG. 14. P-S fold for Orthogonal Design B (sparse shot), interpolated, depth-specific binning

Figure 15 shows that the interpolated P-S fold for the survey geometries defined in Figures 2 and 11 have very similar patterns, although the actual fold in the latter survey is less because there are 30% fewer shots in the survey.

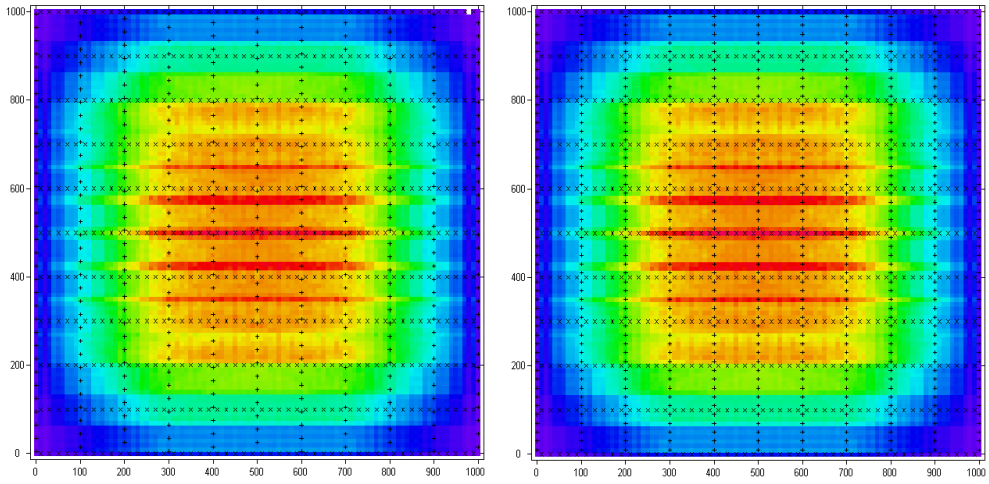

FIG. 15. Comparison between interpolated, depth-specific P-S fold for Orthogonal Designs B (left) and A (right). Design B is the sparse-shot design.

However, the reduced nominal fold is compensated by a significant reduction in traces with non-unique offsets and azimuths, as illustrated by the example shown in Figure 16a, and the offset vs azimuth graph of traces within this particular bin, shown in Figure 16b.

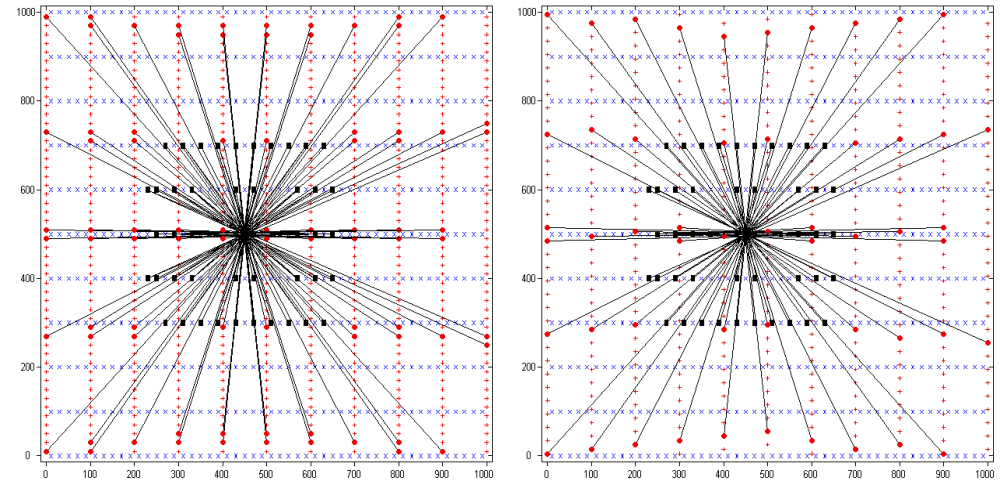

(a)

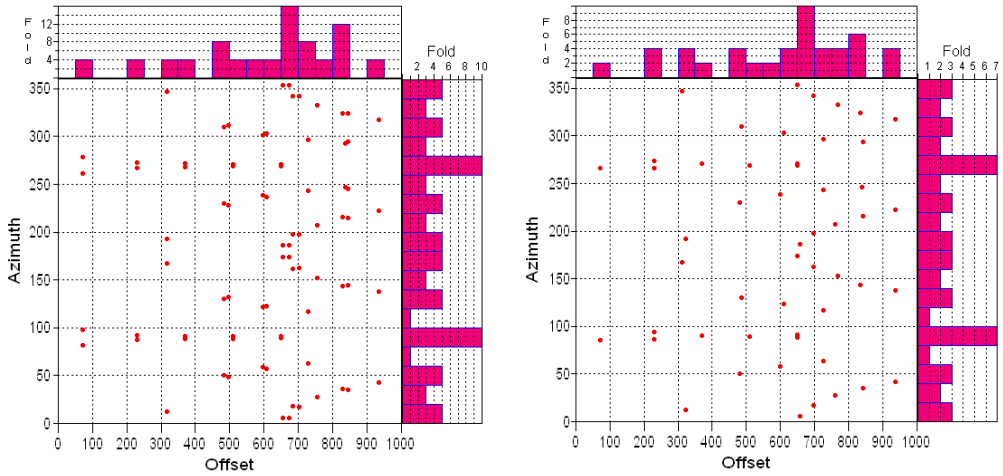

(b)

FIG. 16. (a) map views of P-S rays contributing to an arbitrary bin for Orthogonal Design A (left) and sparse-shot Orthogonal Design B (right); (b) offset versus azimuth plots for the rays in (a). The histograms show offset and azimuth fold in 50 m offset panels and 20^0 azimuth sectors.

Offset and azimuth quality measures

In any P-S (or P-P) survey, a systematic distribution of source-receiver offsets within each bin gather is desired. If the survey objective is to map subsurface fractures, then a wide range of source-receiver azimuths is optimum. Generally, orthogonal or slant surveys will have a better azimuth distribution than swath surveys. Various statistical measures are employed in commercial survey design software packages that show offset and azimuth distributions within bins. In this paper, a new measure of the quality of offset and azimuth distributions within bins is developed by dividing the total offset into

a number of user-defined offset panels, and by dividing the 360^0 of available source-receiver azimuths into a number of user-defined azimuth sectors. The quality of the offset or azimuth distribution is determined from the number of offset panels or azimuth sectors that contain at least one trace; e.g. if all offset panels contain at least one trace, then the offset distribution quality (ODQ) is unity. Similarly, if all azimuth sectors contain at least one trace, then the azimuth distribution quality (ADQ) is unity. The sensitivity of the ODQ or ADQ measures can be increased by simply increasing the number of offset panels or azimuth sectors that are used to assess the distributions. An overall, integrated offset and azimuth survey quality factor (SQF) is also defined, and is given by:

$$SQF = [ODQ * ADQ]^{1/2}.$$

Examples of ODQ, ADQ and SQF maps for orthogonal design B are shown in Figures 17 through 19 respectively.

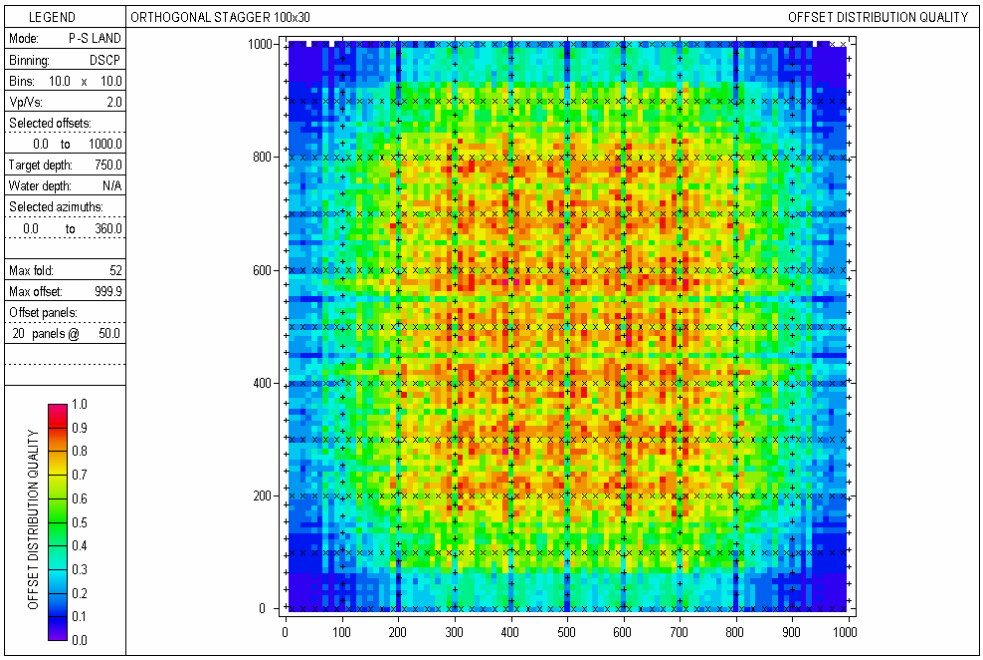

FIG. 17. P-S offset distribution quality factor for the sparse-shot orthogonal survey (Orthogonal Design B). Depth-specific binning.

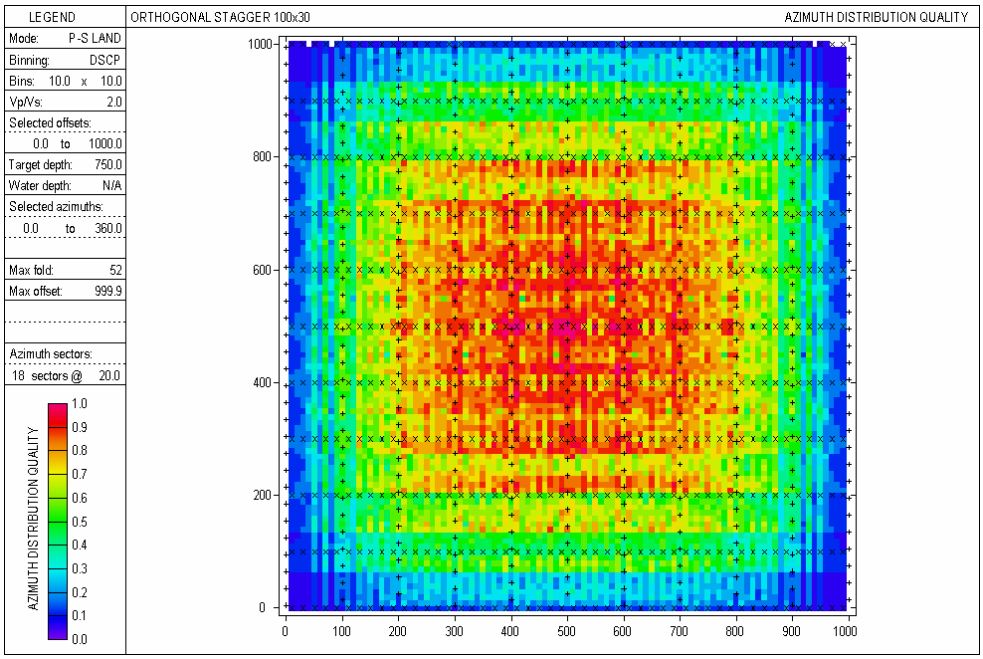

FIG. 18. P-S azimuth distribution quality factor for the sparse-shot orthogonal survey (Orthogonal Design B). Depth-specific binning.

Quality factors in the central part of the survey area a good, although a survey footprint of reduced quality factors is evident.

Figure 20 shows the geometry for Slant Design B, in which the source interval along the shot lines was also increased to 30 m. In Figure 21, the P-P fold for this survey is compared with P-P fold for Orthogonal Design B (30 m shot interval and 10 m stagger). These fold maps are quite similar although some stripes parallel to the receiver lines are evident. Nominal and interpolated P-S fold shown in Figures 22 and 23 respectively, with comparable results. Offset distribution, azimuth distribution and overall survey quality factors for the two survey designs were also compared, with results displayed in Figures 24 through 26, respectively. Again, the results between the survey designs are quite similar, although the slant design appears to have a reduced acquisition footprint compared to the orthogonal design.

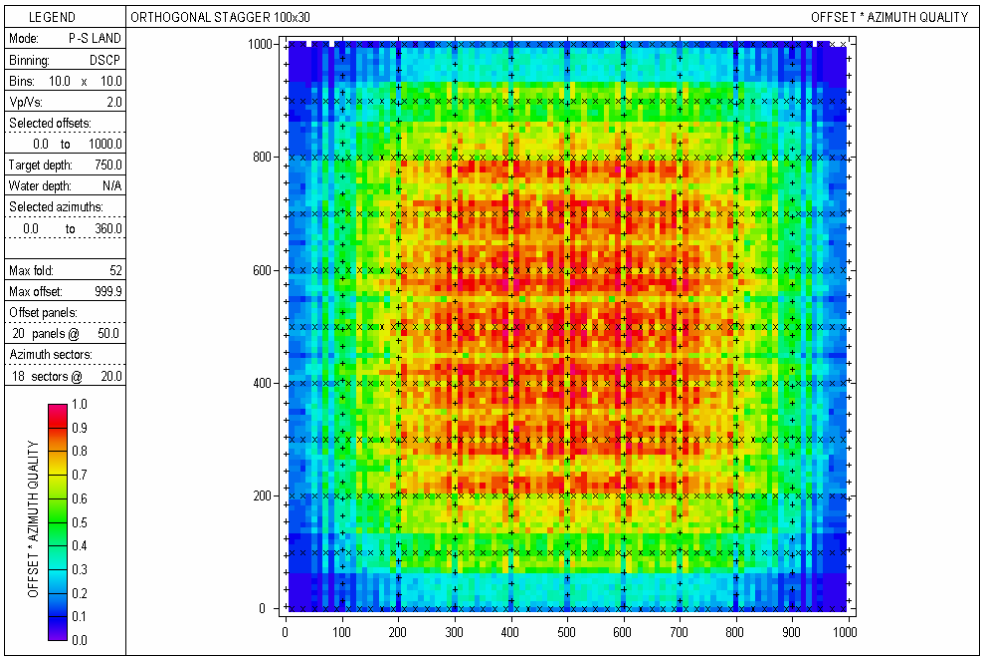

FIG. 19. P-S offset&azimuth survey distribution quality factor for the sparse-shot orthogonal survey (Orthogonal Design B). Depth-specific binning.

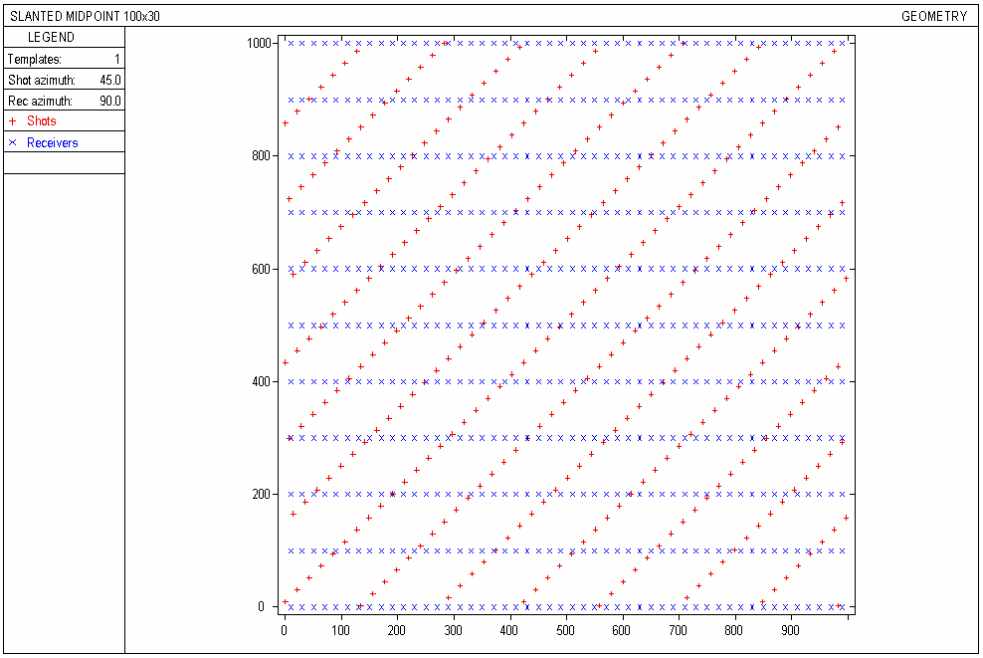

FIG. 20. Slant Design B (sparse-shot). Source interval = 30m; receiver interval = 20m; shot-line interval = receiver-line interval = 100m. Shot-line azimuth = 45^0; receiver-line azimuth = 90^0.

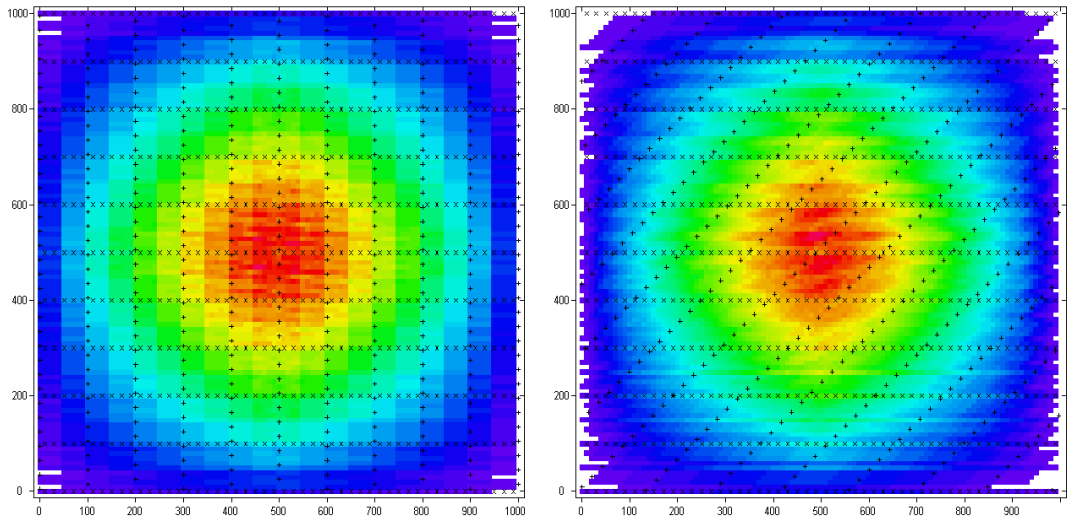

FIG. 21. Comparison between P-P fold for sparse-shot surveys; Orthogonal Design B (left) and Slant Design B (right). Similar fold patterns are observed for the two survey designs although the slant design shows minor striping parallel to the receiver lines.

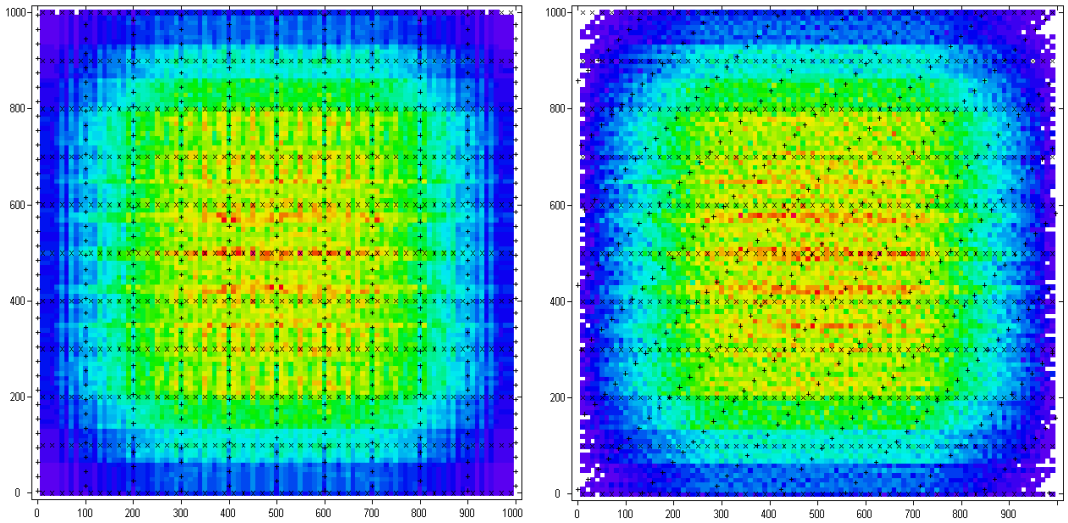

FIG. 22. Comparison between depth-specific P-S fold for sparse-shot surveys; Orthogonal Design B (left) and Slant Design B (right). Similar fold patterns are observed for the two survey designs although the slant design shows slightly greater striping parallel to the receiver lines.

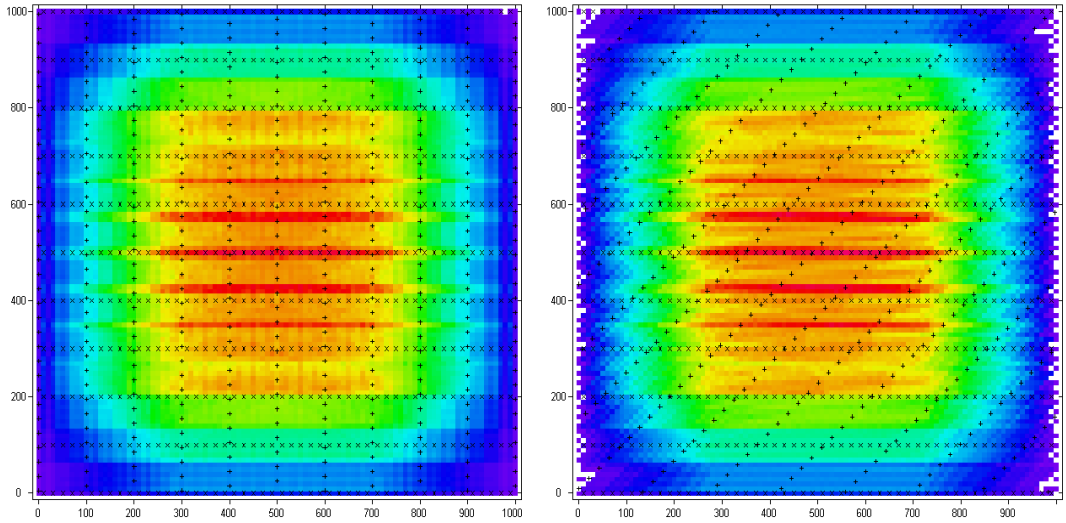

FIG. 23. Comparison between interpolated, depth-specific P-S fold for sparse-shot surveys; Orthogonal Design B (left) and Slant Design B (right). Similar illumination patterns are observed for the two survey designs.

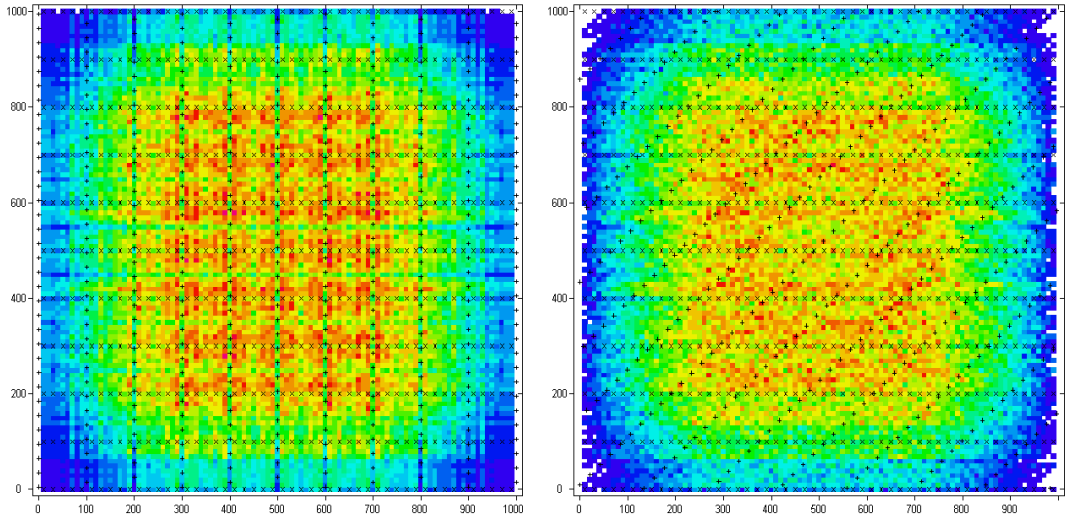

FIG. 24. Comparison between offset distribution quality factors for sparse-shot surveys; Orthogonal Design B (left) and Slant Design B (right). Quality factor increases towards the red end of the spectrum. The orthogonal design shows a greater acquisition footprint than the slant design.

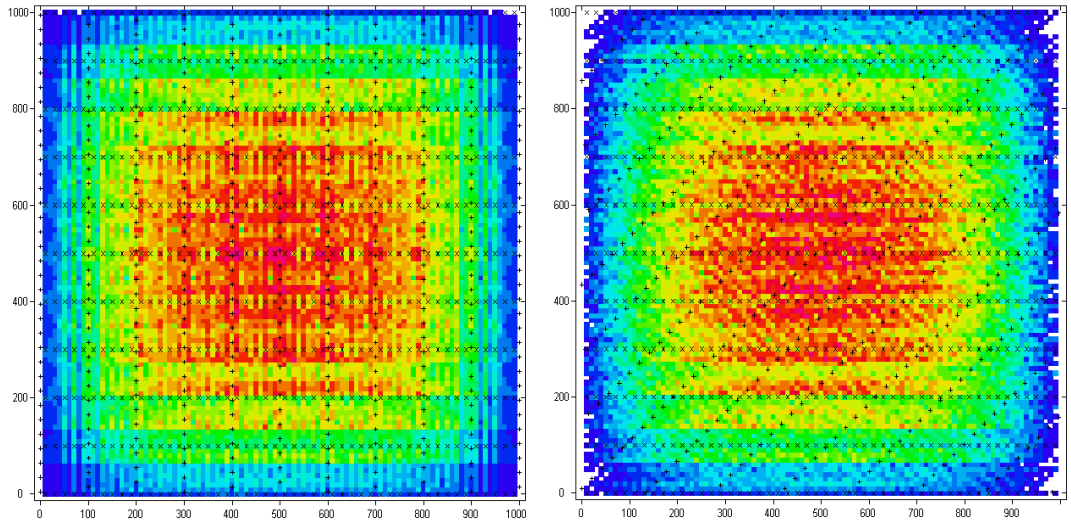

FIG. 25. Comparison between azimuth distribution quality factors for sparse-shot surveys; Orthogonal Design B (left) and Slant Design B (right). Quality factor increases towards the red end of the spectrum. Surveys show similar azimuth quality.

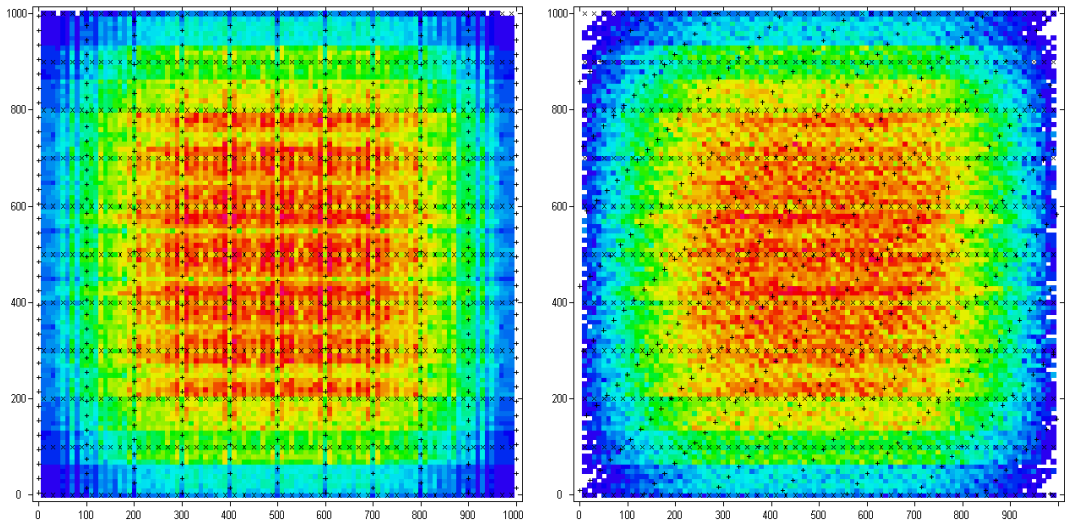

FIG. 26. Comparison between offset&azimuth survey quality factors for sparse-shot surveys; Orthogonal Design B (left) and Slant Design B (right). Quality factor increases towards the red end of the spectrum. The orthogonal design shows a slightly greater acquisition footprint than the slant design.

OBC EXAMPLE

The design approach used for the land orthogonal survey was also tested for an orthogonal ocean-bottom-cable (OBC) survey covering an area of 4km x 3km, a water depth of 100m, and *Vp/Vs* = 2.2. A conventional design, OBC Design A, is illustrated in Figure 27, with fixed receiver cables separated by 150m and shot lines separated by 200m. Shot and receiver intervals are both 50m. In OBC Design B (Figure 28), the shot interval is increased to 75m but the shot line interval is reduced to 133m so that the total source effort is the same in both surveys. In OBC Design B, a shot stagger of 25 m is incorporated to regularize the P-P fold. Receiver configurations are identical in both OBC surveys.

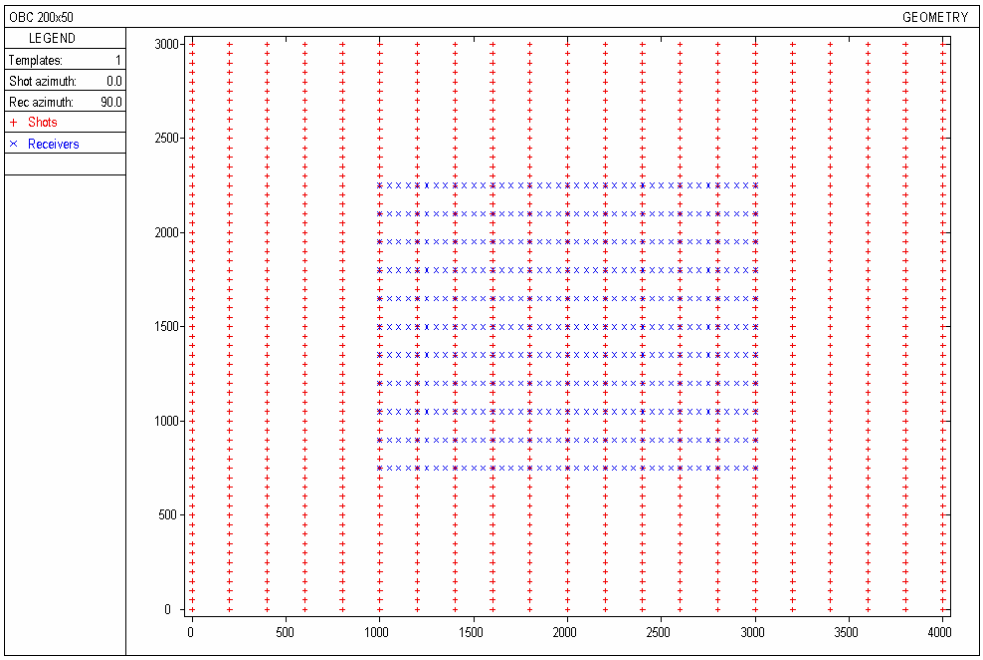

FIG. 27. OBC Design A. Source interval = receiver interval = 50m. Shot-line interval = 200m; receiver-line interval = 150m.

Figures 29 and 30 compare depth-specific P-S fold for a target depth of 3000m. Maximum offset in the design was limited to 4km. Both fold maps are very similar, although some minor fold striping is seen in OBC Design B (Figure 30). SQF maps for both surveys are shown in Figures 31 and 32 with OBC Design B showing a small advantage. However, projected rays for a bin near the centre of the survey area show many closely paired traces for OBC Design A (Figure 33) compared to OBC Design B (Figure 34). This is shown graphically in Figure 35 which plots offset versus azimuth for all traces within the selected bin on each survey, with a greater number of unique traces in OBC Design B.

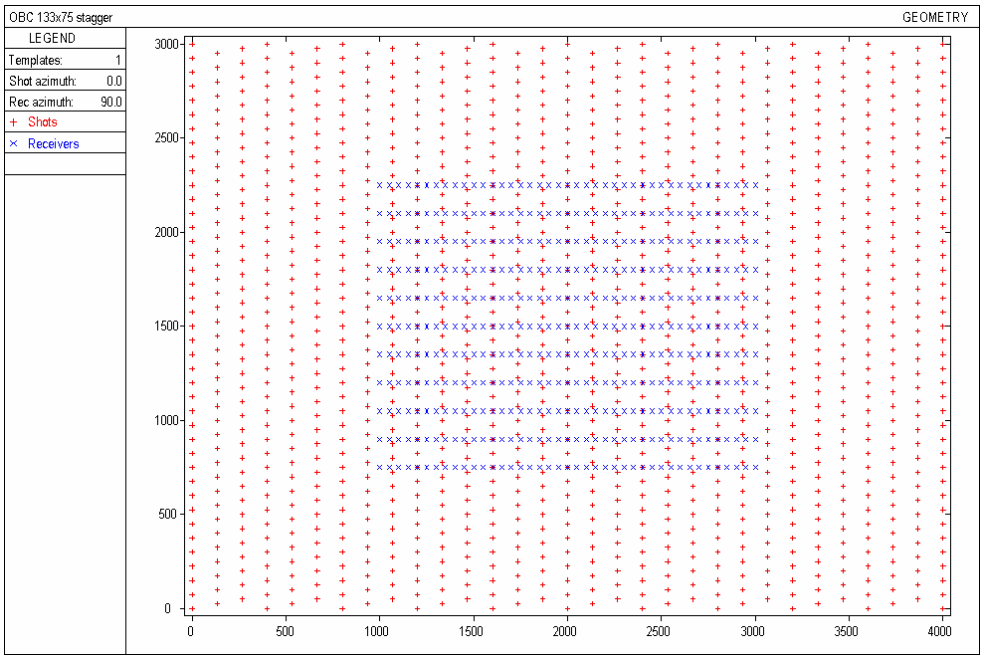

FIG. 28. OBC Design B (sparse-shot). Source interval = 75m; source stagger = 10m; receiver interval = 50m; shot-line interval = 133m; receiver-line interval = 150m.

DISCUSSION

This study has introduced several new concepts in survey design, particularly for converted waves, that are ready to be tested. The close separation of conversion points in the cross-line direction of a 3C-3D survey means that the shot interval should be greater than the receiver interval in order to maximize the distribution, in offset and azimuth, of traces within bins. Good P-P fold distribution can be maintained by adding a shot stagger to adjacent shot lines. New measures of offset and azimuth distribution quality are also introduced in this paper. These measures yield a colour-coded quality factor that can be viewed over the entire survey area.

Orthogonal and slant designs were tested with the new sparse-shot approach and evaluated using the newly derived quality measures. Both surveys were shown to yield similar results with neither design being clearly superior. An OBC design was also evaluated and the sparse shot design is superior to the conventional design with regular shot spacing.

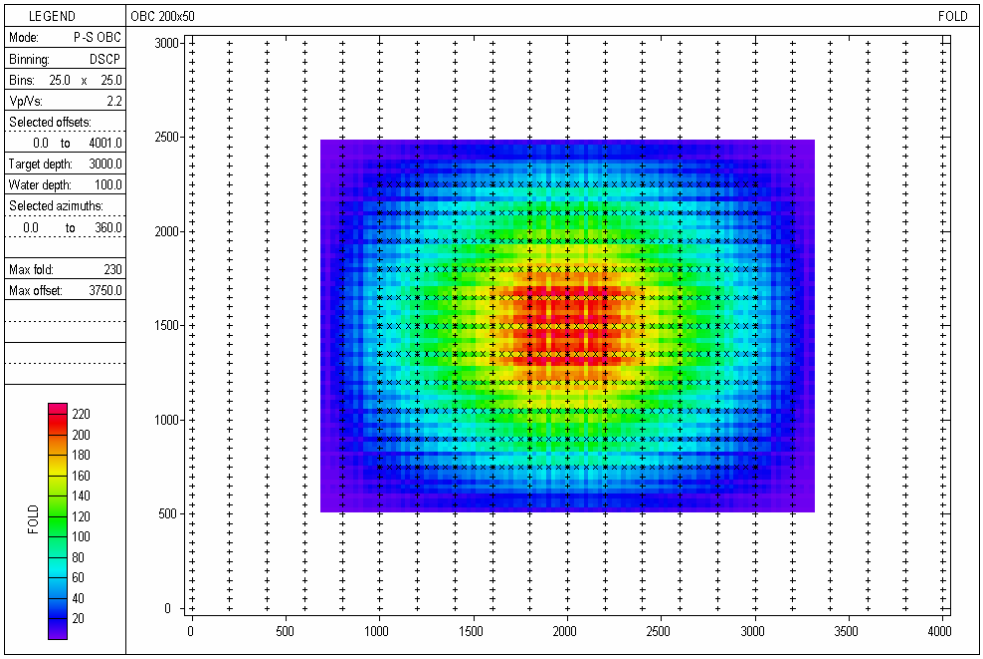

FIG. 29. P-S fold for OBC Design A, depth-specific binning.

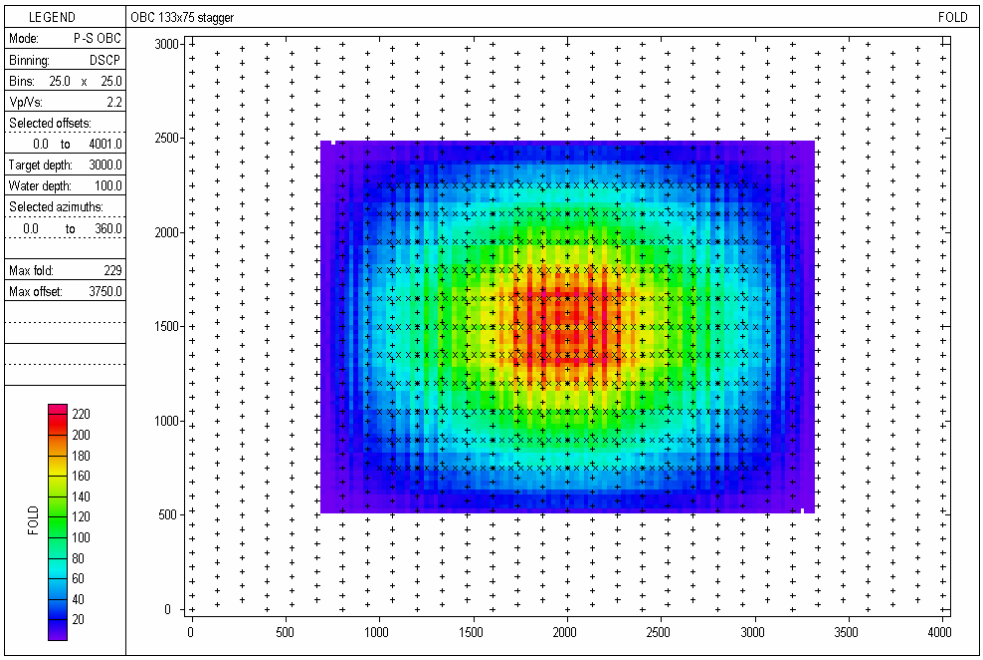

FIG. 30. P-S fold for OBC Design B (sparse-shot), depth-specific binning.

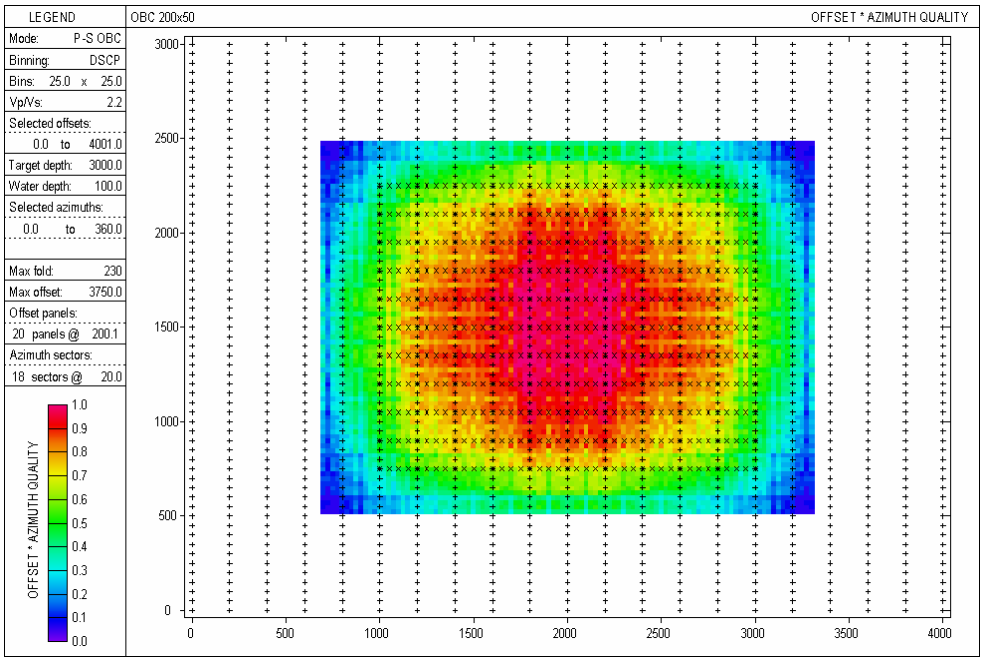

FIG. 31. Offset&azimuth survey quality factor for OBC Design A.

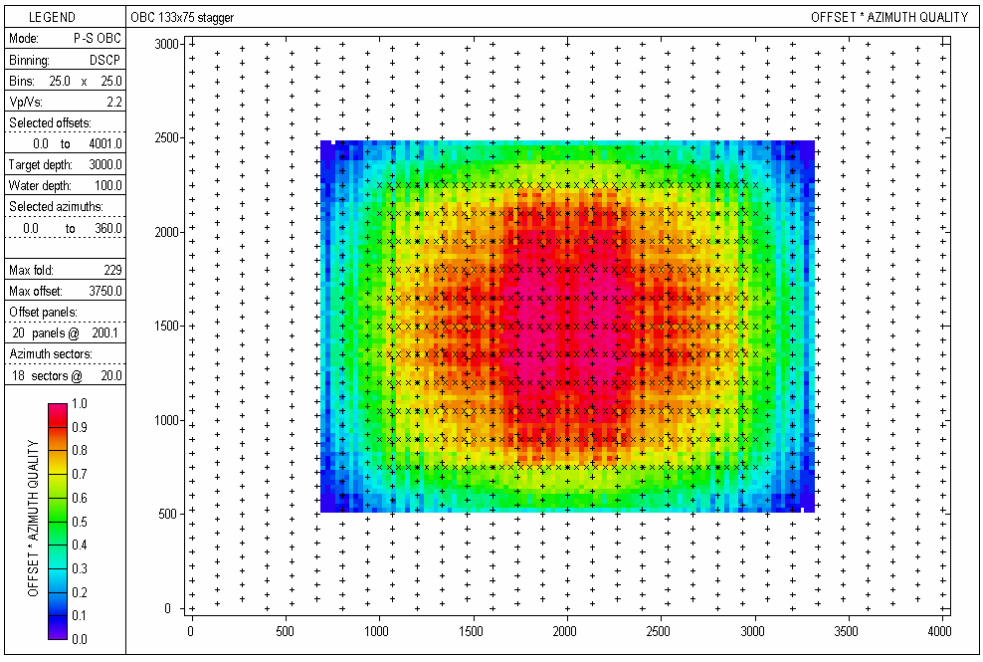

FIG. 32. Offset&azimuth survey quality factor for OBC Design B (sparse-shot).

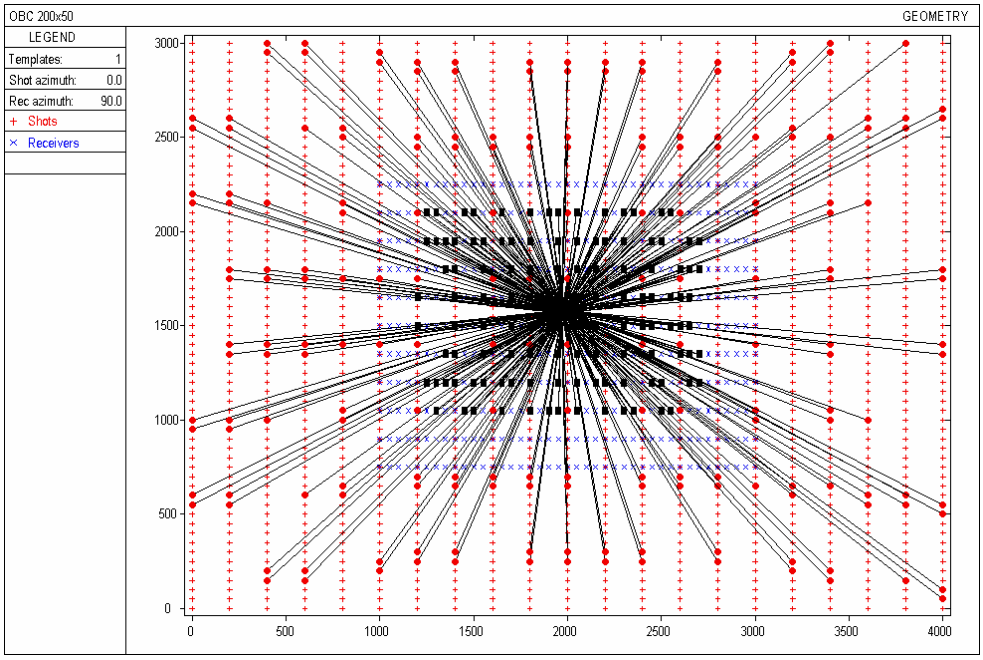

FIG. 33. Map view of P-S rays contributing to an arbitrary bin for OBC Design A. Source-points are denoted by the red dots and receivers are denoted by the black rectangles. Note proximal ray pairs from adjacent shots along common shot lines.

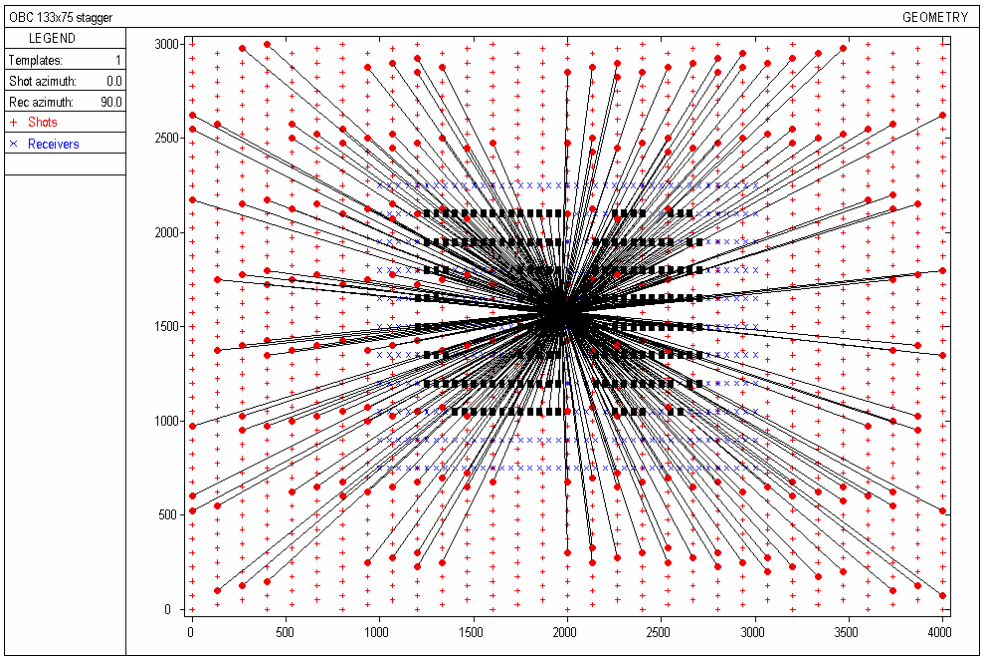

FIG. 34. Map view of P-S rays contributing to an arbitrary bin for OBC Design B (sparse-shot). Source-points are denoted by the red dots and receivers are denoted by the black rectangles. Note fewer proximal rays from adjacent shots along common shot lines than for OBC Design A.

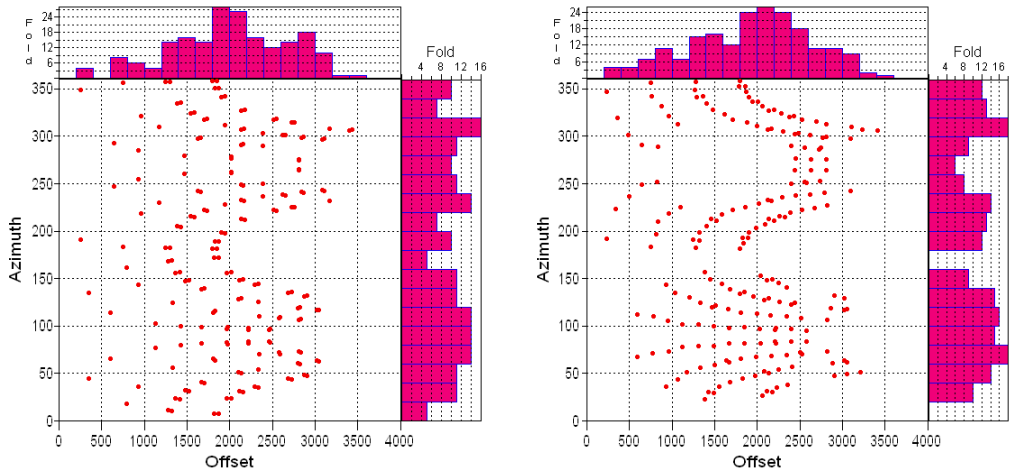

FIG 35. Offset versus azimuth plots for trace data in bins shown in Figures 33 and 34. OBC Design A (left) and OBC Design B (sparse-shot, right). The histograms show offset and azimuth fold in 50 m offset panels and 20^0 azimuth sectors.

ACKNOWLEDGEMENTS

We thank the sponsors of the CREWES Project for financial support.

REFERENCES

Cary. P.W., and Lawton, D.C., 2003, Filling in the gaps in our understanding of converted-wave fold: CSEG Recorder, **28**, No. 8., 32-34.

Cordsen, A, Galbraith, M., and Peirce, J., 2000, Planning land 3-D seismic survyes, Geophysical Developments No. 9, Hardage, B.A., ed., Society of Exploration Geophysicists.

Cordsen, A., and Lawton, D.C., 1996, Designing 3-component 3D seismic surveys: 66th Annual Meeting of the Society of Exploration Geophysicists, Expanded Abstracts, 81-83.

Musser, James A., 2003, Seismic survey designs for converted wave: Annual Joint Conventional of the CSPG and CSEG, Calgary, June 206, 2003.

Yang, J. and Lawton, D.C., 2002, Mapping the P-S conversion point in Vertical Transversely Isotropic(VTI) media , 72nd Ann. Internat. Mtg: Soc. of Expl. Geophys., 1006-1009.

Yang, J. and Lawton, D.C, 2003, Comparison of two P-S conversion point mapping approaches in media exhibiting polar anisotropy, 73rd Ann. Internat. Mtg: Soc. of Expl. Geophys.